ARTICLE

A hybrid bioorganic interface for neuronal photoactivation

Diego Ghezzi[1,*], Maria Rosa Antognazza[2,*], Marco Dal Maschio[1], Erica Lanzarini[2,3],
Fabio Benfenati[1] & Guglielmo Lanzani[2,3]

A key issue in the realization of retinal prosthetic devices is reliable transduction of information carried by light into specific patterns of electrical activity in visual information processing networks. Soft organic materials can be used to couple artificial sensors with neuronal tissues. Here, we interface a network of primary neurons with an organic blend. We show that primary neurons can be successfully grown onto the polymer layer without affecting the optoelectronic properties of the active material or the biological functionality of neuronal network. Moreover, action potentials can be triggered in a temporally reliable and spatially selective manner with short pulses of visible light. Our results may lead to new neuronal communication and photo manipulation techniques, thus paving way to the development of artificial retinas and other neuroprosthetic interfaces based on organic photodetectors.

[1] Department of Neuroscience and BrainTechnologies, Istituto Italiano di Tecnologia, Via Morego 30, Genova 16163, Italy. [2] Center for Nano Science and Technology @Polimi, Istituto Italiano di Tecnologia, via Giovanni Pascoli, 70/3, Milano 20133, Italy. [3] Politecnico di Milano, Physics Department, P.za L. da Vinci 32, Milano 20133, Italy. *These authors contributed equally to this work. Correspondence and requests for materials should be addressed to F.B. (email: fabio.benfenati@iit.it) or G.L. (email: guglielmo.lanzani@iit.it).

Interfacing artificial functional materials and living neuronal tissues is at the forefront of bionanotechnology[1]. Attempts so far have been based on microscale processing of metals, inorganic semiconductors as electrodes[2] or photoactive layers in biased devices[3,4], and more recently, nanomaterials have been investigated[5,6]. However, in spite of extensive research, the communication between biological tissues and artificial sensors is still a challenge. Constraints exist in the complexity of the fabrication processes (that is, metal and semiconductor lithography) and the mechanical properties of the implanted sensing/recording elements (poor flexibility and biocompatibility) that could elicit deleterious tissue reactions such as inflammation and gliosis. In addition, electrodes have fixed geometries that limit the location in space of the stimulus, and electrical currents are often detrimental to the overall system.

In this respect, organic soft matter has potential in terms of flexibility, favourable mechanical properties and biological affinity[7–10]. The use of semiconducting polymers has been reported in mechanical actuators for precise delivery of neurotransmitters[11], and in biosensors[12,13], such as pH and glucose sensors, in which their ability to support mixed ionic/electronic charge transport was fully exploited. Conversely, organic polymers have been tested as coatings of conventional electrodes[14–18] in direct neuronal interfaces for recording and stimulating neuronal activity, whereas the exploitation of their appealing optoelectronic features has never been considered for neuronal communication and photo manipulation devices.

Here, we report the functional interfacing of an organic semiconductor with a network of cultured primary neurons and successfully demonstrate the physiological stimulation of neuronal cells in a network by shaping visible light pulses at the polymer/electrolyte interface. This new approach to the optical stimulation of neurons may stimulate further work towards the development of an artificial retina based on organic materials.

Results

Realization of the bioorganic interface. The active layer of the interface is the prototype material for organic photovoltaic applications[19], namely, regio-regular poly(3-hexylthiophene-2,5-diyl) with phenyl-C61-butyric-acid-methyl ester (rr-P3HT:PCBM) (Fig. 1a). In the bulk heterojunction structure, rr-P3HT works as an electron donor material, whereas PCBM is the electron acceptor, thus ensuring very high external quantum efficiency in the charge generation process[20].

The device was realized through a multi-stage process: the active polymer film was spin-coated onto a glass substrate pre-coated with indium-tin oxide (ITO), which works as the anode of the photodetector, and then the organic blend was annealed at 120 °C for 2 h. The thermal treatment had a double role: it improved the morphology of the polymeric film, enhancing the efficiency of charge photogeneration[21], and it prepared the film for subsequent cell culture by removing all residual traces of organic solvents (for example, acetone, methyl alcohol, chlorobenzene, which are highly toxic for the biological systems) and by sterilizing the substrate. The polymer layer was covered by poly-L-lysine (PLL) to improve adhesion, and primary rat embryonic hippocampal neurons were finally seeded and grown on it.

Assessment of the organic semiconductor functionalities. Specific requirements have to be fulfilled by a successful device based on organic semiconductors: the organic semiconductor must withstand sterilization procedure; the organic semiconductor must preserve its characteristics once immersed in culture medium; cell growth and survival must be demonstrated on top of the organic active layer; and proper functionalities of the semiconducting layer and of the neuronal network have to be demonstrated.

To address the first two issues, we investigated prototypes without neurons, which had undergone the same fabrication steps[22]. We used hybrid solid–liquid devices (Fig. 1b) maintained before the experiment in minimum essential medium (a standard and widely used culture medium) and using an aqueous solution of sodium chloride (NaCl) as the electrolytic cathode. Given that NaCl represents the main ionic content of any extracellular fluid, the latter solution was used as a simpler and proper model system for understanding the hybrid photodetector operation principle. Figure 1c demonstrates that the photosensing capabilities of the organic polymer[20] are fully preserved after thermal sterilization, casting of PLL and direct contact with saline solutions for 12 days. Figure 1d and e show the temporal stability and photostability of the hybrid cell, respectively. We verified that the active polymer blend maintains its photoconversion capability unaltered for 28 days in response to light, while remaining completely immersed in the electrolytic solution for the whole period (Fig. 1d). Moreover, we also verified the effect of a continuous illumination for more than 28 h on the photoconversion efficiency and found that, after a transient decay at the very onset of the illumination, the photocurrent values were very stable over time (Fig. 1e).

Polymer effect on cell viability. To address the issue of biocompatibility of the organic layer, primary neurons were grown for up to 28 days *in vitro* (DIV) onto either PLL-treated ITO/rr-P3HT:PCBM devices (polymer) or control glass substrates covered with ITO and PLL only (control; Fig. 2a). Neuronal adhesion to the substrate and growing pattern on ITO/rr-P3HT:PCBM devices were virtually identical under both conditions. To compare the cell viability on ITO/rr-P3HT:PCBM devices with respect to control substrates, propidium iodine/fluorescein diacetate staining was carried out at various times in culture (Fig. 2b). No significant differences were found in both cell viability (Fig. 2c, $P = 0.558$, one-way analysis of variance (ANOVA), $n = 6$) and mortality under both culture conditions (Fig. 2d, $P = 0.445$, one-way ANOVA, $n = 6$), indicating that the organic polymer alters neither the network development nor the neuronal viability over a long period of time.

Polymer effect on neuronal physiology. The physiological properties of neurons cultured on bioorganic active interfaces were evaluated by using the standard patch-clamp technique. Both the resting membrane potential (Fig. 3a) and the frequency and amplitude distribution of spontaneous excitatory postsynaptic currents (Fig. 3b) were closely similar under the two culture conditions. Moreover, the firing rate measured in current-clamp mode (Fig. 3c) did not reveal any significant difference between the two conditions. To characterize network behaviour under the two conditions, neurons were plated onto microelectrode array biochips and the network mean firing rate was measured after 21 DIV[23] (Fig. 3d). No differences in spontaneous network firing were observed between uncoated and polymer-coated multielectrode arrays (*t*-test, $P = 0.843$, $n = 9$). These results demonstrate that organic layers are highly biocompatible and fully preserve the fundamental physiological characteristics of mature neurons.

Neuronal photostimulation. We tested the performance of the interface structure as an intercommunication device by evaluating the efficacy of light excitation to trigger the activity of whole-cell patched neurons (Fig. 4a). Whole-cell recordings were carried out (Fig. 4b) under photostimulation in photovoltaic mode ($V_b = 0$ V). First, we checked that the photostimulation mechanism did not affect the cellular microenvironment. When the extracellular pH was monitored in close proximity to the recorded cells in the presence or absence of photostimuli, the local pH did not significantly drift over 0.02 pH units (Fig. 4c), a change which is unlikely to affect neuronal function. Moreover, a deterministic correspondence between photostimulation of the organic semiconductor close to the cell body and neuronal activation was found (Fig. 4d). Spike
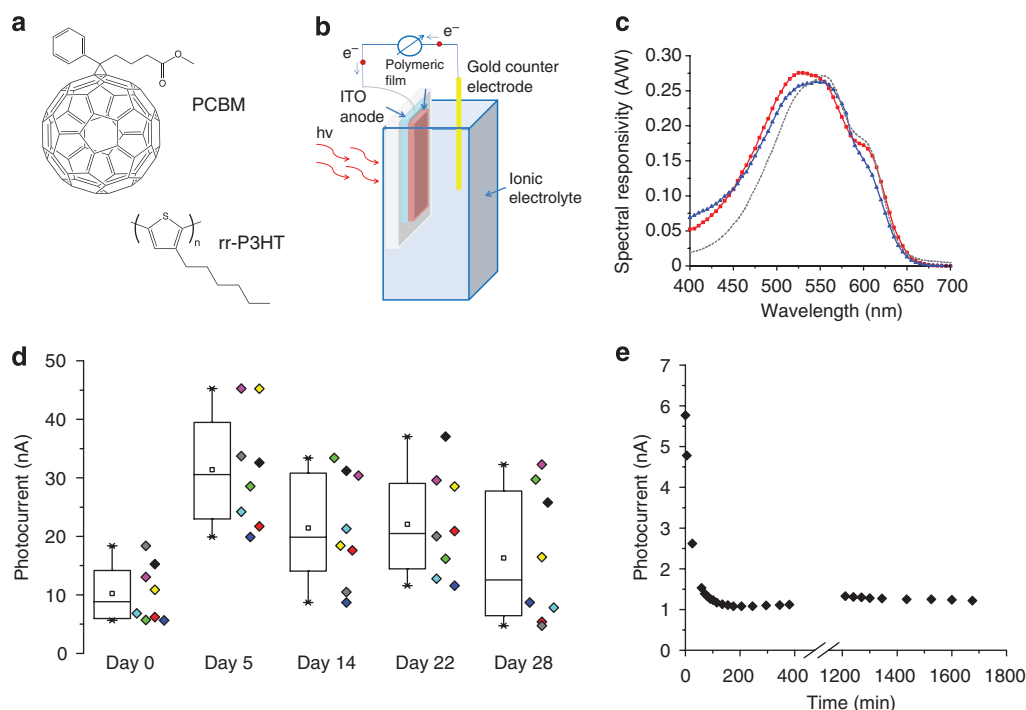
Figure 1 | Operation principle of the solid–liquid organic photodetector. (**a**) Chemical structures of regio-regular poly(3-hexylthiophene-2,5-diyl) (rr-P3HT) and phenyl-C61-butyric-acid-methyl ester (PCBM). (**b**) Scheme of the hybrid solid–liquid cell for modulated photocurrent spectroscopy. (**c**) Spectral response of the systems ITO/rr-P3HT:PCBM/NaCl/Gold (blue line and triangles) and ITO/rr-P3HT:PCBM/Ringer/Gold (red line and squares), with the saline solutions working as ionic cathodes, recorded after 12 days of immersion in minimum essential medium. Typical spectral response (in arbitrary units for direct comparison with present results) of a conventional, solid-state solar cell (ITO/rr-P3HT:PCBM (1:1)/Al) is reported as a reference (dashed, grey line). Minor changes in the spectrum shape have to be ascribed to slightly different sample thicknesses and processing conditions[20]; however, one should note that main spectral features are well reproduced. (**d**) Photocurrent maxima (at 530 nm) recorded from eight distinct devices (represented in different colours by diamond symbols) immediately after fabrication (day 0) and up to 28 days later. Samples were kept completely immersed in the electrolyte for the whole period. Box plot limits represent the 25th and 75th percentile and whiskers represent the outliers (coefficient 1.5) of the distribution. The mean (square), maximum and minimum values of the distribution are also shown. (**e**) Stability of the photocurrent of the system ITO/rr-P3HT:PCBM/NaCl/Gold on continuous illumination. The data show the photocurrent recorded at 530 nm at various times up to 28 h.
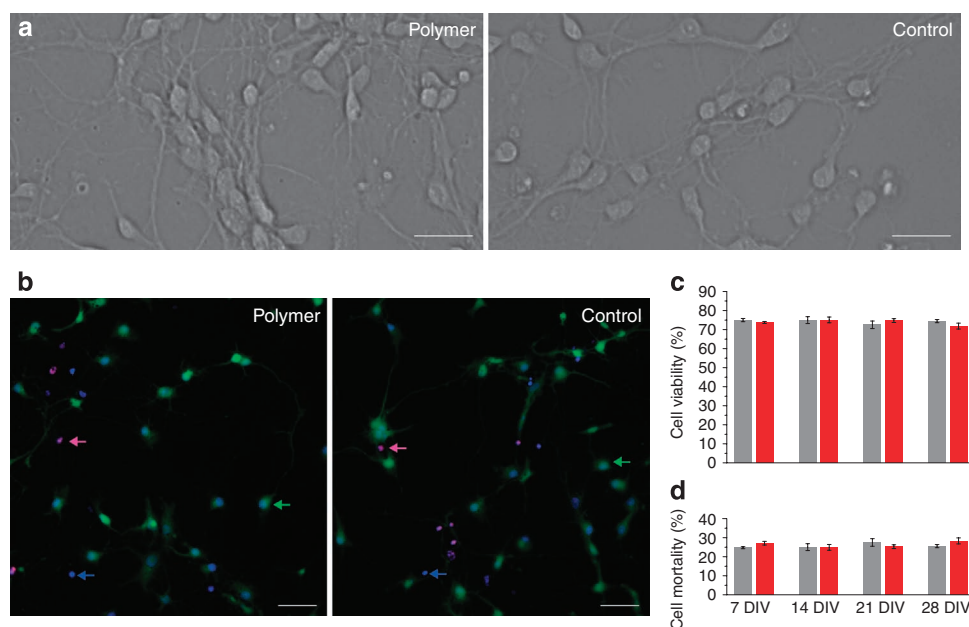

Figure 2 | Cell viability on bioorganic active interface. (**a**) Hippocampal neurons cultured on either poly-L-lysine (PLL)-treated ITO/rr-P3HT:PCBM devices (left) or control glass substrates covered with ITO and PLL only (right) after 12 DIV. Scale bars, 25 μm. (**b**) Propidium iodine/fluorescein diacetate staining assay carried out at 21 DIV. Green, blue and violet arrows indicate viable cells, apoptotic cells and necrotic/apoptotic cells, respectively. Scale bars, 25 μm. (**c**) Statistical analysis of cell viability on control (grey) or polymer-coated (red) substrates ($P = 0.558$, one-way ANOVA, $n = 6$) at four time points: 7 DIV, 14 DIV, 21 DIV and 28 DIV. (**d**) Statistical analysis of cell mortality ($P = 0.445$, one-way ANOVA, $n = 6$) at the same time points of panel (**c**).
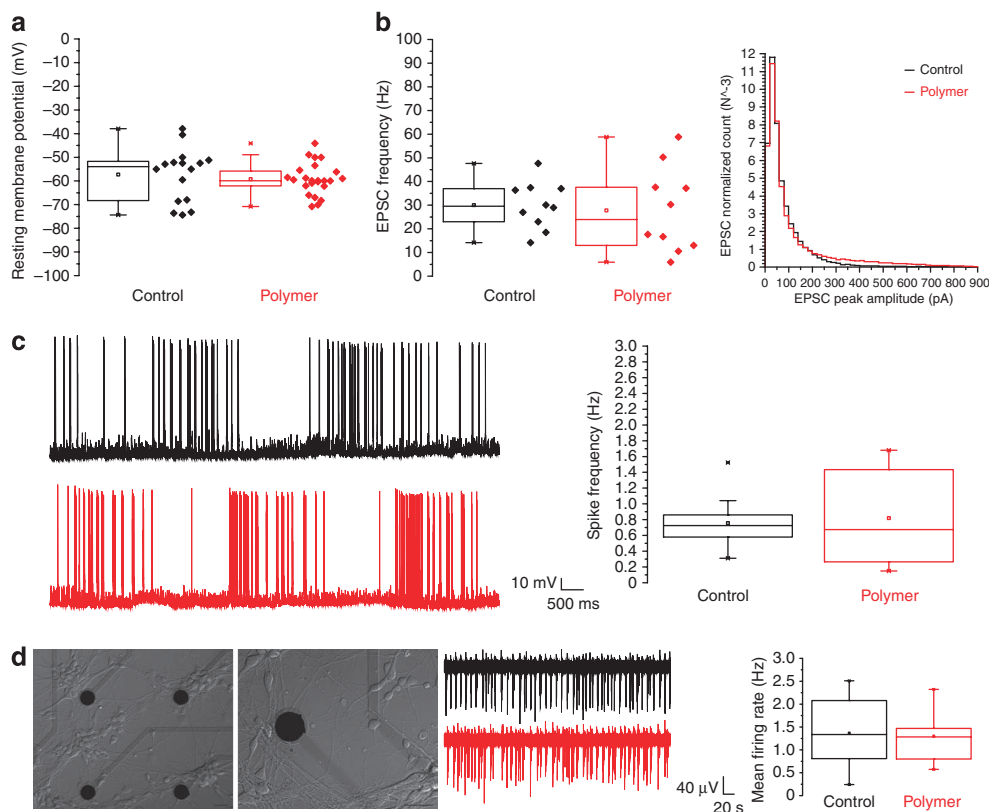
Figure 3 | Spontaneous electrical activity of primary hippocampal neurons cultured onto bioorganic active interfaces. (**a**) The resting membrane potential of neurons cultured on either poly-L-lysine (PLL)-treated ITO/rr-P3HT:PCBM devices (red, $n=24$) or control glass substrates covered only with ITO and PLL (black, $n=16$) was measured (t-test, $P=0.506$). (**b**) Analysis of the frequency (left; t-test, $P=0.736$, $n=10$) and amplitude distribution (right; $n=6$, bins 20 pA) of spontaneous excitatory postsynaptic currents (EPSCs). (**c**) Example of whole-cell recordings from neurons cultured on either polymer (red) or control (black) substrates. The analysis of neuronal firing rates in ITO/rr-P3HT:PCBM devices (red, $n=10$) and control substrates (black, $n=10$) did not show any significant difference (left, t-test, $P=0.780$). (**d**) Network mean firing rates (MFRs) computed with multielectrode array devices. Sample traces show a representative example of extracellular spikes recorded in the presence (red) or absence (black) of polymer deposition. Statistical analysis (t-test, $P=0.843$, $n=9$) did not show any difference between the two conditions. Scale bars, 30 μm. Box plot limits represent the 25th and 75th percentile and whiskers represent the outliers (coefficient 1.5) of the distribution. The mean (square), maximum and minimum values of the distribution are also shown.

trains (Fig. 4e, upper panel) could be elicited with trains of light pulses (20 ms at 1 Hz) with a negligible percentage of failures (< 15% on the total number of delivered pulses; see Fig. 4e bottom panel). Single spikes were rapidly and precisely evoked (time to peak: 11.324±0.171 ms; jitter: 1.481±0.258 ms). The spatial selectivity of photostimulation was investigated by aligning a 3×3 stimulation grid to the neuronal cell body of each optically stimulated neuron ($n=10$) under whole-cell recording (Fig. 4f, left). Peristimulus time histograms show that action potentials were reliably evoked only when the stimulus spot was precisely hitting the cell body, whereas the stimulus was virtually ineffective when the spot was translated by a cell body diameter in all directions (Fig. 4f, right).

Discussion
The physical mechanism underlying the photostimulation process (Fig. 4g) could be either a pure resistive (R_i) behaviour or a pure capacitive (C_i) behaviour, or a combination of the two. In the first scenario[24], following polymer photoexcitation and photocurrent generation, the charge migration from the polymer to the electrolyte gives rise to Faradaic currents; subsequently, the ionic imbalance created in the extracellular medium can give rise to membrane depolarization and subsequent firing. This scenario is usually taken into consideration whenever an external bias, stronger than the relevant electrochemical potentials and high enough to enable water hydrolysis (in our case higher than 3.4 V), is applied. Note

that Faradaic processes resulting from reduction–oxidation electrochemical reaction between species in solution and electrodes might induce both electrode damage and cell degradation, and for this reason these processes should be avoided. The photostimulation configuration relying on a pure capacitive mechanism is characterized by the generation of two oppositely charged Helmholtz layers at the electrolyte/polymer and neuronal membrane/electrolyte interfaces, without charge transfer processes between the polymer and the electrolyte[25]. A charge displacement within the polymeric bulk induces ion redistribution at the electrolytic/cell membrane interface, thus leading to membrane depolarization with subsequent action-potential generation.

Considering that the device operates in photovoltaic mode, the recorded photocurrent is low (in the order of hundreds of pA) and as we did not observe any adverse effect during the stimulation experiments (neither modification of the polymeric film, nor of the neuronal culture), the capacitive coupling is the most likely mechanism of stimulation. Although a Faradaic component of the current cannot be completely excluded, in our case it seems to be negligible; if present, a significant increase in the concentration of hydroxide ions is expected, in contrast to our experimental evidence.

In conclusion, we demonstrate a new communication protocol between organic semiconductors and neuronal cells showing photostimulation of neuronal activity. Our approach has advantages with respect to similar attempts based on biased devices[3,4]. In contrast
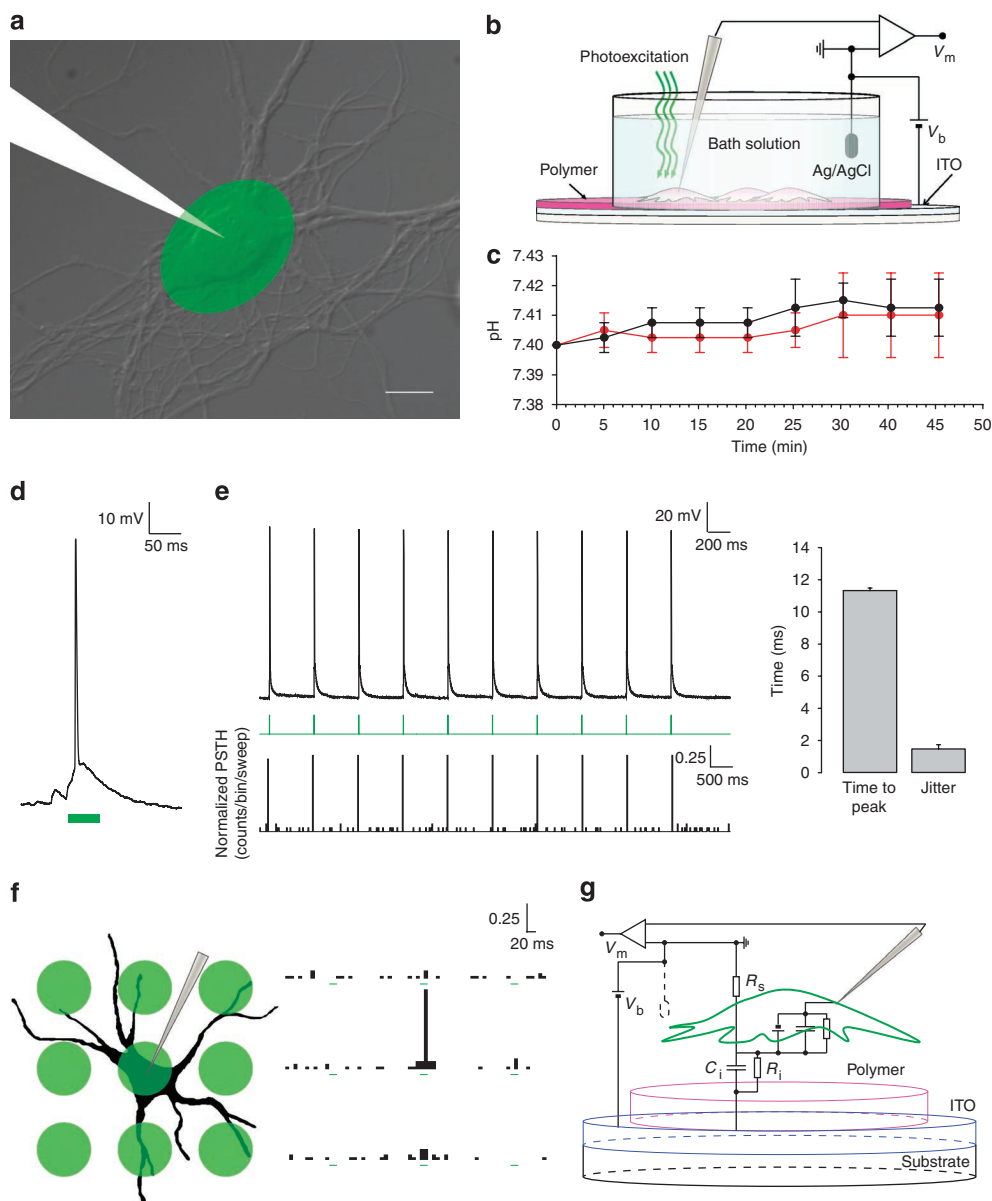
Figure 4 | Optical stimulation of neurons cultured onto an ITO/rr-P3HT:PCBM device. (**a**) Schematic representation of the optical stimulation paradigm including the localization of the stimulus in a region surrounding the patched neuron (scale bar, 10 μm). (**b**) Scheme of the photosensing interface, with the neuronal network grown on top of the polymer active layer during patch-clamp recordings. (**c**) Online monitoring of pH of the extracellular solution during the experiments in the presence (black, $n = 4$) or absence (red, $n = 4$) of photostimulation. Data are presented as means±s.e.m. (**d**) Action-potential generation in response to a photostimulation pulse (50 ms). (**e**) Example of spike train generated with 20 ms pulses repeated at 1 Hz (upper panel). Peristimulus time histogram (PSTH) count was computed and normalized by considering spike trains in all recorded neurons (bottom panel; $n = 10$, bins 20 ms). The right plot shows (means±s.e.m.) the latency to the spike peak with respect to the light onset computed by averaging all spikes in the train obtained from all recorded neurons and the jitter calculated as the s.d. of spike latencies measured across all recorded neurons ($n = 10$). (**f**) Spatial properties of the photostimulating interface. A grid of nine spots (diameter 20 μm, spacing 30 μm) was overlaid to a patched neuron and spikes were counted. PSTHs, arranged in a similar grid, represent the spike counts normalized for the total number of sweeps in all recorded neurons ($n = 10$, bins 10 ms). Each histogram represents the count of the spikes recorded at the soma by the corresponding stimulation spot. (**g**) Model of the polymer/electrolyte and electrolyte/neuron interface, where C_i and R_i represent the capacitance and the resistance of the double layer at the interface of electrolyte and polymer, respectively. V_b represents the bias voltage traditionally applied for the cell stimulation (in our case $V_b = 0$), R_s the electrolyte resistance and V_m the measured membrane potential. Green bars and traces represent light pulses in all panels.

to metal or silicon interfaces, the proposed interface works without any externally applied electric field and with minimal heat dissipation, favourably addressing the thermal issues, which are extremely relevant in an efficient biological interface.

It was demonstrated that by using organic semiconductors one can closely reproduce the colour response functions of the human retina[26]; this work suggests that π-conjugated materials can be taken into consideration for a new generation of biomimetic artificial retinal prostheses. Organic technology is characterized by simple and cheap fabrication techniques; existing deposition methods such as ink-jet printing, allow the realization of a variety of geometrical patterns with various active areas, up to few square micrometres, thus offering the possibility to specifically target selected groups of cells.

The use of soft matter provides some advantages in terms of mechanical properties, as it enables the production of light, thin and flexible devices, better suited to implantation within a

biological environment. Moreover, in terms of photoconversion efficiency, as recently discussed[27,28], the appropriate stimulatory light to induce polymeric photostimulation can be obtained and modulated by using a combination of camera detectors and light emitters as enhancers (MicroLEDs)[29], thus ensuring that the retinal prosthetic device can work in a wide-band range of ambient light intensities.

The present approach represents a new tool for neural active interfacing, which is a simpler alternative to the existing and widely used neuron optogenetic photostimulation techniques[30], and avoids gene transfer, which is potentially hazardous. The photostimulation is not specific for selected neuronal populations, as is this case for genetically encoded approaches, but the optical stimulation of neurons could be micrometrically shaped to stimulate selected neuronal populations owing to the high spatial selectivity of the photostimulation interface, and could lead to the development of new artificial optoelectronic neurointerfaces based on biocompatible organic materials.

Methods

Semiconducting polymers. Both rr-P3HT and PCBM were supplied by Sigma-Aldrich and used without any further purification. rr-P3HT has a regio-regularity of 99.5% and molecular weight of $17,500\,g\,mol^{-1}$. An accurate cleaning of the substrate was required: the substrate was rinsed in an ultrasonic bath with, subsequently, a specific tension-active agent in water solution (HELLMANEX II, 3%), deionized water, pure acetone and isopropyl alcohol. Oxygen plasma cleaning of the substrate completed the process. 1,2-Chlorobenzene solutions of P3HT and PCBM were prepared separately, with a concentration of $7.5\,g\,l^{-1}$, and then mixed together (1:1 volume ratio) using a magnetic stirrer. The solution was then heated at 50 °C, stirred and finally deposited on the ITO-covered (thickness 0.4 mm) glass substrate, previously heated, by spin coating. Spinning parameters (first step: 800 r.p.m., angular acceleration $1,500\,rad\,s^{-2}$, rotation duration 2 s; second step: 1,500 r.p.m., angular acceleration $4,000\,rad\,s^{-2}$, rotation duration 30 s) were carefully selected to obtain suitable optical quality and film thickness (~150 nm). Polymers on ThinMEA200/30 (Multi Channel Systems MCS GmbH) were deposited in the same way. After deposition, organic layers were annealed and properly sterilized by heating at 120 °C for 2 h. Control substrates (ITO-covered glass substrates) were properly sterilized in the same way.

Photocurrent measurement. In the modulated photocurrent spectroscopy, a 30-W halogen tungsten lamp that served as a source of white light, filtered through a monochromator before being focused on the polymer film. The light was chopped by a mechanical chopper, whose reference signal was fed to a lock-in amplifier with detection at the chop frequency (270 Hz). All measurements were taken at room temperature without applying bias. The hybrid device had a vertical geometry with an ITO layer that served as an anode, the active polymer deposited on top of it, and an aqueous NaCl (200 mM) solution used as the electrolytic liquid cathode. Other solutions tested for the cathode included: minimum essential medium, recording extracellular solution (Ringer, see below) and several aqueous solutions with various concentrations of other salts like NaI or NaBr. The photocurrent was extracted and measured in the external circuit through a counter-electrode (gold) immersed in the electrolyte.

Cell culture preparations. Primary cultures of hippocampal neurons were prepared from embryonic 18-day rat embryos (Charles River), as previously described[31]. Briefly, hippocampi were dissociated by a 15-min incubation with 0.25% trypsin at 37 °C, and cells were plated at a density of 275–300 cells per mm^2 on PLL ($0.1\,mg\,ml^{-1}$)-treated organic layers or control substrates in Neurobasal (Invitrogen) supplemented with 10% Horse serum (Hyclone). ThinMEA200/30 (Multi Channel Systems MCS GmbH) were treated with PLL and neurons were plated at a density of 400–500 cells per mm^2. After allowing neurons to adhere to the surface for 3–4 h, cells were cultured in serum-free Neurobasal supplemented with 2% B27 (Invitrogen), 2 mM Glutamine (Invitrogen) and 1% Penicillin/streptomycin mixture (Invitrogen).

Cell viability assay. Cell viability was verified by propidium iodine/fluorescein diacetate staining at 7 DIV, 14 DIV, 21 DIV and 28 DIV. Attached cells were rinsed twice with Ringer and incubated for 4 min in Ringer containing $15\,\mu g\,ml^{-1}$ of Fluorescein diacetate (Sigma-Aldrich), $5\,\mu g\,ml^{-1}$ of Propidium iodine (Sigma-Aldrich) and $3\,\mu g\,ml^{-1}$ of Hoechst-33342 (Sigma-Aldrich). Cells were washed with Ringer and multiple images were taken by a C91006 CCD Camera (Hamamatsu Photonics Italia) mounted on a Nikon Ti-E epifluorescence microscope (Nikon Instruments). Standard 4′-6-diamidino-2-phenylindole (ex: D350/50x, em: D460/50m, dic: 400dclp), fluorescein isothiocyanate (ex: D480/30x, em: D535/40m, dic: 505dclp) and tetramethylrhodamine isothiocyanate (ex: D540/25x, em: D605/55m, dic: 565dclp) filter sets were used to image Hoechst-33342, fluorescein diacetate and propidium iodine, respectively.

At each time point, images were taken from both organic layers ($n=6$) and control substrates ($n=6$). Five fields per substrate were imaged and the percentage of living (or dead) cells per field was counted and averaged. The percentage of healthy cells was calculated as the percentage of cells expressing fluorescein diacetate on the total nuclei expressing Hoechst-33342. As a control, the percentage of dead cells was computed as the percentage of apoptotic cells (identified by Hoechst-33342) and necrotic cells (identified by propidium iodine) on the total number of nuclei expressing Hoechst-33342. Percentage of living cells (or dead cells) was reported at every time point as mean±s.e.m. of six independent plates.

Electrophysiology. Electrophysiology was performed on a setup based on a Nikon FN1 upright microscope (Nikon Instruments). Differential interference contrast (DIC) images were taken by a C91006 CCD Camera (Hamamatsu Photonics Italia). Whole-cell patch-clamp recordings were performed between 14 DIV and 18 DIV at room temperature using patch pipettes (4–6 MΩ), under GΩ patch sealing, using an Axopatch 200B (Axon Instruments). The recording extracellular solution (Ringer) contained (mM): NaCl 135, KCl 5.4, $MgCl_2$ 1, $CaCl_2$ 1.8, HEPES 5, glucose 10 and pH was adjusted to 7.4 with NaOH. The intracellular solution contained (mM): KCl 140, HEPES 5, EGTA 5, $MgCl_2$ 2 and pH was adjusted to 7.35 with KOH. Responses were amplified, digitized at 20 kHz and stored with pCLAMP 10 (Axon Instruments). Further analyses were carried out using pCLAMP 10 and Matlab (The MathWorks).

Excitatory postsynaptic currents were recorded in voltage-clamp mode by applying a −70-mV holding. Peaks were detected in 5 min recordings per cell by a threshold algorithm implemented in Matlab. ESPCs distribution was normalized by the area. Single-cell spike frequency was evaluated by 5-min current-clamp recording per cell. Microelectrode array recordings were performed in the culturing medium at 37 °C using the MEA1060-inv-BC system (Multi Channel Systems MCS GmbH). Data recorded at $25\,kHz\,ch^{-1}$ from the 60 channels were filtered from 200 Hz to 3 kHz and spikes were sorted using a threshold algorithm included in the MC Rack software (Multi Channel Systems MCS GmbH). The threshold per every electrode was defined as a multiple of the s.d. of the biological noise computed during the first 500 ms of the recording ($-5\times s.d._{noise}$). Global mean firing rate of the network in a multielectrode array chip was computed as mean of the firing rates obtained for every active channel present in the chip.

pH measurements were taken during electrophysiological experiments, in both organic layers and controls substrates, using a PCE-228 (PCE Italia) pH metre equipped with a BEE-CAL compensator (World Precision Instruments) and a Beetrode wire pH electrode (World Precision Instruments). Data are always presented as mean±s.e.m.

Photostimulation. Using a custom LabView application (National Instruments), a specific region of interest surrounding the soma of a selected neuron was drawn and the resulting binary image was used to control a Digital Micromirror Device (DMD, Texas Instruments). The DMD was in turn used to shape a Laser beam (Cobolt) resulting in a selective photostimulation limited to the defined region of interest. Laser pulses (532 nm, $10\,mW\,mm^{-2}$) were timed using a Mechanical shutter (Uniblitz) and delivered to the sample through a 40×/0.8NA water immersion objective (Nikon Instruments).

Statistical analysis. Statistical analysis was carried out using SigmaPlot (Systat Software), and data were plotted using OriginPro (OriginLab Corporation) softwares. Data were compared by Student's t-test or one-way ANOVA.

References

1. Wallace, G. G., Moulton, S. E. & Clark, G. M. Electrode-cellular interface. *Science* **324,** 185–186 (2009).
2. Kipke, D. R. Advanced neurotechnologies for chronic neural interfaces: new horizons and clinical opportunities. *J. Neurosci.* **28,** 11830–11838 (2008).
3. Starovoytov, A., Choi, J. & Seung, S. Light-directed electrical stimulation of neurons cultured on silicon wafers. *J. Neurophysiol.* **93,** 1090–1098 (2005).
4. Goda, Y. & Colicos, M. A. Photoconductive stimulation of neurons cultured on silicon wafers. *Nat. Protoc.* **1,** 461–467 (2006).
5. Kotov, N. A. *et al.* Nanomaterials for neural interfaces. *Adv. Mater.* **21,** 3970–4004 (2009).
6. Pappas, T. C. *et al.* Nanoscale engineering of a cellular interface with semiconductor nanoparticle films for photoelectric stimulation of neurons. *Nanoletters* **7,** 513–519 (2007).
7. Dionigi, C. *et al.* Control of neuronal cell adhesion on single-walled carbon nanotubes 3D patterns. *J. Mater. Chem.* **20,** 2213–2218 (2009).
8. Bystrenova, E. *et al.* Neural networks grown on organic semiconductors. *Adv. Funct. Mat.* **18,** 1751–1756 (2008).
9. Isaksson, J. *et al.* Electronic control of Ca^{2+} signalling in neuronal cells using an organic electronic ion pump. *Nat. Mater.* **6,** 673–679 (2007).
10. Wan, A. M. D., Brooks, D. J., Gumus, A., Fischbach, C. & Malliaras, G. G. Electrical control of cell density gradients on a conducting polymer surface. *Chem. Comm.* **35,** 5278–5280 (2009).
11. Simon, D. T. *et al.* Organic electronics for precise delivery of neurotransmitters to modulate mammalian sensory function. *Nat. Mater.* **8,** 742–746 (2009).

12. Owens, R. M. & Malliaras, G. G. Organic electronics at the interface with biology. *MRS Bull.* **35,** 449–456 (2010).
13. Roberts, M. E. *et al.* Water-stable organic transistors and their application in chemical and biological sensors. *Proc. Natl Acad. Sci. USA* **105,** 12134–12139 (2008).
14. Guimard, N. K., Gomez, N. & Schmidt, C. E. Conducting polymers in biomedical engineering. *Prog. Polym. Sci.* **32,** 876–921 (2007).
15. Gomez, N., Lee, J. Y., Nickels, J. D. & Schmidt, C. E. Micropatterned polypyrrole: a combination of electrical and topographic characteristics for the stimulation of cells. *Adv. Funct. Mat.* **17,** 1645–1653 (2007).
16. Richardson-Burns, S. M. *et al.* Polymerization of the conducting polymer poly(3,4-ethylenedioxythiophene) (PEDOT) around living neural cells. *Biomaterials* **28,** 1539–1552 (2007).
17. Widge, A. S., Jeffries-El, M., Cui, X., Lagenaur, C. F. & Matsuoka, Y. Self-assembled monolayers of polythiophene conductive polymers improve biocompatibility and electrical impedance of neural electrodes. *Biosens. Bioelectron.* **22,** 1723–1732 (2007).
18. Asplund, M., Von Holst, H. & Inganas, O. Composite biomolecule/PEDOT materials for neural electrodes. *Biointerphases* **3,** 83–93 (2008).
19. Günes, S., Neugebauer, H. & Sariciftci, N. S. Conjugated polymer-based organic solar cells. *Chem. Rev.* **107,** 1324–1338 (2007).
20. Dennler, G., Scharber, M. C. & Brabec, C. J. Polymer-fullerene bulk-heterojunction solar cells. *Adv. Mater.* **21,** 1323–1328 (2009).
21. Campoy-Quiles, M. *et al.* Morphology evolution via self-organization and lateral and vertical diffusion in polymer:fullerene solar cell blends. *Nat. Mater.* **7,** 158–164 (2008).
22. Antognazza, M. R., Ghezzi, D., Musitelli, D., Garbugli, M. & Lanzani, G. A hybrid, solid-liquid polymer photodiode for the bio-environment. *Appl. Phys. Lett.* **94,** 243501–243503 (2009).
23. Chiappalone, M., Bove, M., Vato, A., Tedesco, M. & Martinoia, S. Dissociated cortical networks show spontaneously correlated activity patterns during *in vitro* development. *Brain Res.* **1093,** 41–53 (2006).
24. Fromherz, P. Electrical interfacing of nerve cells and semiconductor chips. *Chem. Phys. Chem.* **3,** 276–284 (2002).
25. Schoen, I. & Fromherz, P. The mechanism of extracellular stimulation of nerve cells on an electrolyte-oxide-semiconductor capacitor. *Biophys. J.* **92,** 1096–1111 (2007).
26. Antognazza, M. R., Scherf, U., Monti, P. & Lanzani, G. Organic-based tristimuli colorimeter. *Appl. Phys. Lett.* **90,** 163509–163511 (2007).
27. Cepko, C. Neuroscience. Seeing the light of day. *Science* **329,** 403–404 (2010).
28. Busskamp, V. *et al.* Genetic reactivation of cone photoreceptors restores visual responses in retinitis pigmentosa. *Science* **329,** 413–417 (2010).
29. Degenaar, P. *et al.* Optobionic vision—a new genetically enhanced light on retinal prosthesis. *J. Neural. Eng.* **6,** 035007 (2009).
30. Miesenböck, G. The optogenetic catechism. *Science* **326,** 395–399 (2009).
31. Kaech, S. & Banker, G. Culturing hippocampal neurons. *Nat. Protoc.* **1,** 2406–2415 (2006).

Acknowledgments

Author contributions
D.G. and M.R.A. contributed equally to this work. G.L. and F.B. conceived and planned the experiments. M.R.A. and E.L. prepared the polymer films and performed the photocurrent experiments. D.G. prepared primary neuronal cultures and performed the cell viability assay. D.G. and M.D.M. performed all the electrophysiological experiments. M.R.A. and D.G. wrote the main paper together with G.L. and F.B. All authors discussed the results and commented on the manuscript at all stages.

Additional information
Competing financial interests: The authors declare no competing financial interests.

Reprints and permission information is available online at http://npg.nature.com/reprintsandpermissions/

How to cite this article: Ghezzi, D. *et al.* A hybrid bioorganic interface for neuronal photoactivation. *Nat. Commun.* 2:166 doi: 10.1038/ncomms1164 (2011).